Title
CROSS SECTIONS FOR ELECTRON CAPTURE BY FAST PROTONS IN H2, He, N2, AND Ar

Authors
Welsh, Leland M.
Berkner, Klaus H.
Kaplan, Selig N.
et al.

Publication Date
1966-12-09

UCRL-16765 Rev.

University of California

Ernest O. Lawrence Radiation Laboratory

CROSS SECTIONS FOR ELECTRON CAPTURE BY FAST PROTONS IN H_2, He, N_2, AND Ar

Berkeley, California

DISCLAIMER

Submitted to the Physical Review

UCRL-16765 Rev.
Preprint

UNIVERSITY OF CALIFORNIA

Lawrence Radiation Laboratory
Berkeley, California

AEC Contract No. W-7405-eng-48

CROSS SECTIONS FOR ELECTRON CAPTURE BY FAST PROTONS IN H_2, He, N_2, AND Ar

Leland M. Welsh, Klaus H. Berkner, Selig N. Kaplan, and Robert V. Pyle

December 9, 1966

Cross Sections for Electron Capture by Fast Protons in H_2, He, N_2, and Ar*

Leland M. Welsh,† Klaus H. Berkner, Selig N. Kaplan, and Robert V. Pyle

Lawrence Radiation Laboratory
University of California
Berkeley, California

December 9, 1966

ABSTRACT

Cross sections for electron capture by protons have been measured at energies from 440 keV to 13.8 MeV in N_2 and in Ar; to 5.41 MeV in He; and to 2.45 MeV in H_2. Electron-loss cross sections in the same gases at 1.027 and 2.44 MeV are also presented.

The measurements were carried out by analysis of particle-beam composition after exit from a gas target of known composition and thickness. The beam was separated magnetically, and the charged and neutral components were detected by a Faraday cup and a scintillator, respectively.

The energy range of our results overlaps that of Barnett and Reynolds between 440 keV and 1 MeV. Our electron-capture cross sections in this region agree within the experimental uncertainty for H_2 and He, but are larger by up to 50% in N_2 and Ar.

I. INTRODUCTION

In this research we investigate the charge-exchange process in which a high-energy proton picks up an electron from an atom or molecule of a target gas and emerges as a neutral hydrogen atom. Early calculations, both classical[1] and quantum-mechanical,[2] of cross sections for such reactions did not prove completely satisfactory. For that matter, the asymptotic (high-energy) behavior of the cross sections has not yet been completely resolved.

There have been many subsequent refinements and variations of the early calculations involving various approximation schemes, some of which are mentioned in the section dealing with theoretical development. These calculations have usually produced results which, in the high-energy limit, vary either as $E^{-11/2}$ or as E^{-6}.

Experimental results to energies of approximately 100 keV are available from several sources.[3] Barnett and Reynolds extended the measurements to 1 MeV;[4] above 1 MeV measurements have been limited to isolated points.[5,6]

The present work concerns charge-exchange measurements for protons in hydrogen, helium, nitrogen, and argon gases. Ranging in proton energy from 440 keV to as high as 13.8 MeV (in N_2 and Ar) these measurements provide a bridge between the previous data below 1 MeV and the few higher-energy points. The experimental technique was similar to one employed previously,[5] but two accelerators were required to accommodate the measured energy range, a 1-MeV Van de Graaff at the low end and the 90-inch cyclotron at Lawrence Radiation Laboratory (LRL), Livermore at the high end. (Two of the points reported, He at 2.99 and 5.41 MeV, were measured at the Hilac at LRL, Berkeley.)

II. RESUME OF APPLICABLE THEORY

Many various approaches to the calculation of the cross section for capture of electrons by fast protons in gases have been made without completely resolving the questions of magnitude or of energy dependence at high energies. Some discussion of the philosophies of these calculations may be found in the book of Mott and Massey,[7] in the articles by Bransden and Cheshire[8] and by Mittleman,[9] and in the reviews by Bates and McCarroll[10] and by Bransden.[11] For purposes of comparison with experiment we list some of the published theoretical predictions about electron capture at high energies.

A. Classical Impulse Approximation

The earliest electron-capture calculations were carried out by Thomas in the classical impulse approximation.[1] For a light projectile incident on a heavy atom he obtained a capture cross section proportional to $E^{-11/4}$; if the target is also a light atom the energy variation is $E^{-11/2}$.

Bates and Mapleton have recently rederived the results of Thomas and, for heavy target atoms, have remarkably improved the agreement between the calculations and experiments at the lower energies ($\lesssim$ 100 keV) by changing a limit of integration.[12] They also point out that Thomas' calculation could be improved at high energies by using better electron distribution functions. The result would be to lower the cross section at very high energies.

For light target atoms, Bates and Mapleton have shown that the Thomas derivation is probably incorrect and that this model predicts an energy dependence at high projectile speeds of $E^{-9/2}$ rather than $E^{-11/2}$.

However, they conclude that the classical approach may not be suited to the case of capture from light atoms, a conclusion reached in another way by Cook.[13]

Estimates based on classical considerations also have been made by Bohr[14] and by Gryzinski.[15] Bohr estimated that the high-energy capture cross sections in heavy target gases should vary as E^{-3}; Gryzinski states that he would not expect his calculations to be good at high energies.

B. First Born Approximation

Agreeing with Oppenheimer[16] that the interaction between the incident proton and the target nucleus should not contribute to the electron-capture cross section, Brinkman and Kramers[2] obtained a first Born-approximation result, which for ground-state capture in atomic hydrogen is

$$Q_{BK}(H) = \pi a_0^2 \, \frac{64}{5} \, \frac{1}{E(1+E)^5},$$

with E in units of 100 keV. (The notations Q_{BK} and Q_{OBK} for this quantity both occur in the literature.) Capture into excited states is customarily taken into account at high energies[16,17] by multiplying the ground-state cross section by

$$\sum_{n=1}^{\infty} n^{-3} = 1.202.$$

Including this factor, and expressing the energy in MeV, we have

$$Q_{BK}(H) = \frac{1.35\times10^{-21}}{E(0.1+E)^5} \text{ cm}^2,$$

i.e., $Q_{BK} \propto E^{-6}$ at high energies. Brinkman-Kramers type calculations have also been made for atoms of higher Z.[9,18-20] Detailed calculations by Mapleton for nitrogen[19,20] and oxygen[19] show that for energies below about 1 MeV the major contribution to the cross section comes from capture of 2p electrons, whereas at higher energies capture of 1s and 2s electrons predominates. The asymptotic energy dependence for these two processes is E^{-7} and E^{-6}, respectively.

Mittleman[9] has given a simple expression for the total capture cross section

$$Q(Z) = a_0^2 \frac{2^{18}}{5} (1.201)\pi^2 \frac{Z}{E^6} n_A(0)\left[1 + \mathcal{O}\left(\frac{Z^2}{E}\right)\right] ,$$

and has indicated that the approximation should be good over the region $10 < E/Z^2 < 42$, where E is in units of 25 keV, Z is the atomic number of the target atom,[21] and $n_A(0)$ is the electron density at the origin. If E is in MeV and $n_A(0)$ is in atomic units,[22] the cross section is given by

$$Q(Z) = \frac{4.25\times10^{-21}}{E^6} Zn_A(0)\ \text{cm}^2 .$$

The accuracy of this expression is expected to improve with increasing Z.[23]

The first Born-approximation solution, retaining an internuclear potential, is commonly called the "Born" or "Jackson-Schiff" approximation. The result Q_B (sometimes written Q_{JS}), is considerably smaller than Q_{BK} at modest energies, and for hydrogen at high energies[17]

$$Q_B(H) \rightarrow 0.661\ Q_{BK}(H) .$$

Thus Q_B is also proportional to E^{-6} at high energies. The asymptotic limit of the proportionality factor has not been evaluated for other gases, although an approximate calculation by Mapleton for He gives[24]

$$Q_B(\text{He}) \rightarrow 0.535\, Q_{BK}(\text{He}) .$$

Since the calculation of Jackson-Schiff electron-capture cross sections for complex atoms is much more difficult than the calculation of Brinkman-Kramers cross sections, only "crude" estimates[24] of Jackson-Schiff cross sections for N and O have been reported.[19,20] These were obtained by simply multiplying Q_{BK} for these atoms by the ratio Q_B/Q_{BK} for H or He.

C. Second Born Approximation

It is found that, when the next higher term in the Born series is retained, the effect of the internuclear potential cancels identically and in the high-energy limit,[25]

$$Q_{B2}(\text{H}) \rightarrow \left[0.2946 + \frac{5\pi v}{2^{12}}\right] Q_{BK}(\text{H}) ,$$

where v is in atomic units, i.e., Q_{B2} is proportional to $E^{-11/2}$ at sufficiently high energies. In terms of proton energy in MeV, we have

$$Q_{B2}(\text{H}) \rightarrow \left[0.2946 + 0.0242\ \sqrt{E}\right] Q_{BK}(\text{H}) .$$

We should note that the applicability of the Born approximation to the electron-capture problem is questionable, because the Born series may not converge, even at high energies.[25,26]

D. The Quantum Impulse Approximation

A quantum-impulse-approximation calculation by Cheshire[27] gives the result that

$$Q_I(H) \rightarrow \left[0.2946 + \frac{5\pi v}{2^{11}}\right] Q_{BK}(H) ,$$

i.e., the same high-energy limit as the second Born approximation, $Q \sim E^{-11/2}$, except that it is larger by a factor of two. For E in MeV, we have $Q_I(H) \rightarrow (0.2946 + 0.0485 \sqrt{E})\, Q_{BK}(H)$. The results of an impulse approximation calculation by Pradhan and Tripathy[28] are available only in graphical form and are presented later in Fig. 4 of this paper.

E. Other Methods

In the expansion method due to Bates,[29] the total wave function is expanded in a series of atomic wave functions. In lowest order it gives the same results as Q_{BK} for high-energy reactions.[30]

Cheshire's continuum-distorted-wave approximation[31] gives, in first order, the same asymptotic expression as his impulse approximation, $Q_I(H)$; the second-order asymptotic results is the same as $Q_{B2}(H)$.

III. APPARATUS AND PROCEDURE

The details of the apparatus changed slightly between experiments on the different accelerators, but basically the arrangement was as shown in Fig. 1. In order to measure the electron-capture cross section, σ_{10}, a beam of protons of precisely known energy and with a small energy spread was deflected into a gaseous target where some fraction of the protons captured electrons. The charged and neutral components were then separated magnetically. The neutral atoms passed undeflected into a plastic or CsI scintillator, while the charged beam was deflected by 10 deg into a Faraday cup.

The section labeled "neutralizer" in Fig. 1 was used in the determination of the ionization cross section, σ_{01}, which must be known in order to correct for loss of neutrals within the gas cell. These measurements were carried out by inserting a 140-μg/cm^2 aluminum foil into the beam ahead of the gas target and sweeping the charged component out of the beam line so that only the neutral hydrogen atoms entered the gas cell.[32] After passing through the gas cell the charged and neutral components were separated by a magnetic field. In this measurement the intensities of both beams were comparable, and atoms and protons were both recorded by counting scintillation pulses. Since the cross section varies slowly with energy and experimental time was short, we measured σ_{01} at two energies only.

The gas cell was similar to one previously described,[33] with an effective length of 24.4 cm (the center-to-center distance between the 0.5-cm-diam, 4.4-cm-long entrance and exit collimator tubes). The gas pressure in the 10-cm-long differentially pumped sections on each side of the cell was always maintained at less than 0.5% of the target pressure. The drift sections, both before and after the gas cell assembly, are pumped by liquid-nitrogen-trapped 4-in. oil-diffusion pumps. Base pressures were approximately 4×10^{-6} torr in these sections. At each energy and in each target approximately ten different measurements were made over a range of pressures, the maximum pressures being those for which the correction for ionization of neutral atoms within the gas cell amount to 20%.

Pressures in the gas target were monitored with a Schulz-Phelps-type ion gauge (Westinghouse WL7676). This was calibrated against a liquid-nitrogen-trapped McLeod gauge whose mercury was cooled to 0°C in order to effectively eliminate the pumping action of mercury streaming to the cold trap.[34] Random errors in pressure calibration were estimated from the long-time fluctuations in calibration points. The total uncertainty in the gas target thicknesses--compounded of estimated uncertainties in the absolute calibration of the McLeod gauge, the effective length of the gas cell, and the fluctuations in the calibrations--is approximately ± 8%.

The charge collected by the Faraday cup was measured with an integrating electrometer, fed back with a low-leakage Fast capacitor. The system was calibrated with a battery-and-precision-resistor current source, which was independently calibrated with a Keithley 401 electrometer. Secondary electron loss from the cup was prevented by the field of a permanent magnet. We estimate the uncertainty in knowledge of proton-beam magnitude as ±1.5%. The integrating electrometer in conjunction with a Speedomax recorder was used to gate off the scalers counting the neutral beam when some appropriate present charge level was reached.

The neutral beam was detected and counted with a thin-window scintillation-detector assembly. At the higher energies a plastic phosphor was used; however, at energies of 1 MeV and below, we found it desirable to increase our light yield and converted to cesium iodide. The photomultiplier output pulses were counted by scalers, after the discrimination of low-level noise. The pulses produced by beam particles were monochromatic and significantly larger than the noise, so that it was easy to discriminate between noise and true counts. The detector size (1-1/2 in. diam) was chosen to be large enough to capture all of the particles in the beam.

The very strong energy dependence of the electron-capture cross sections demands that the proton beam energies be accurately determined. Three techniques were used: (1) At all energies measurements were made with a lithium-drifted silicon solid-state detector with a maximum depletion depth of 3 mm (which was sufficient to stop the highest-energy particles). This detector was calibrated with 5.477-MeV α particles from Am^{241} both directly and after attenuation by a 0.5 mg/cm^2 aluminum foil. Each energy was measured to an estimated ±1% in this way. (2) At the 90-inch cyclotron, the energies were also measured with a device called a "ranger"[35] which determines the proton range in a set of thin aluminum foils. The uncertainty in this determination is also estimated to be ±1%. (3) The energy calibrations at the 1-MeV Van de Graaff were based on the nuclear reaction $F^{19}(p,\alpha\gamma)O^{16}$ which has resonances at 872.5 and 340.5 keV, and on $Li^7(p,\gamma)Be^8$ at 441.2 keV.[36] These points were used to calibrate the magnetic-field monitor of the momentum-selecting magnet located just before the entrance to the apparatus. An uncertainty of approximately ±3 keV was assigned to these measurements.

IV. DATA ANALYSIS AND RESULTS

A. Calculation of σ_{10} and σ_{01}

The calculation of the capture cross section is facilitated by the fact that the cross sections for the formation of H^- are negligibly small at these energies. Hence we consider only a two-component system consisting of H^0 and H^+. Since the gas target is always thin with respect to the capture reaction, i.e., the mean free path for the capture reaction is very much larger than the target length, we also make the approximation that the total number of particles in the beam is the same as the number of charged particles and obtain the following expression for the electron capture cross section:

$$\sigma_{10} = \frac{[N_0 - n_{b2} - n_{b1}\exp(-\Pi\sigma_{01})]\sigma_{01}}{N_+[1 - \exp(-\Pi\sigma_{01})]},$$

where N_0 and N_+ are the numbers of neutrals and protons measured by the detectors, Π is the target thickness in atoms or molecules per cm^2, σ_{01} is the ionization cross section of neutral hydrogen atoms; n_{b1} is the number of hydrogen atoms entering the gas target chamber due to electron capture on background gas ahead of the target, and n_{b2} is the number of neutrals produced by electron capture from the background gas between the exit of the target chamber and the magnet. In practice we measured only the sum of n_{b1} and n_{b2}, but for purposes of analysis we estimate from geometry and pressure measurements in the regions of interest that n_{b1} is approximately 80% of the total neutral background, and n_{b2} about 20%.

To determine the neutral stripping cross section, σ_{01}, we again use the fact that in our energy range σ_{10} is much less than σ_{01} and obtain the expression

$$\sigma_{01} = \frac{1}{\Pi} \ln\left[1 + \frac{N_+ - n_{b+}}{N_0}\right],$$

where n_{b+} is the background-proton count rate.

B. Errors

The error in σ_{10} results from uncertainties in (1) target thickness, (2) electron-loss cross section, (3) particle-detection efficiency, (4) background, and (5) the effect of impurities.

1. Target Thickness

For each individual cross-section measurement there are small random uncertainties in the relative pressure determinations, perhaps 2%. These contribute negligible error when the ten measurements are combined into a single value of σ_{10} for a given target gas and energy. However as previously mentioned, we believe that there is an absolute systematic uncertainty of about 8% in the target thickness; this is folded into the final results.

2. Electron Loss Cross Section, σ_{01}

The values of σ_{01} used in the calculations were obtained by interpolating between the previously reported measurements[4, 33, 37] and the results reported here. To these we assign errors of ±10%, which typically results in a ±2% uncertainty for most σ_{10} values and, at worst, gives ±5% in H_2 at 2.45 MeV. As previously mentioned, we are not able to accurately assess the value of σ_{01} that is appropriate to the interior of the gas cell,[32] but we assume that the resultant uncertainties in the values of σ_{10} are relatively small.

3. Particle Detection Efficiency

Counting errors are considered to be less than or equal to 1%. The uncertainty assigned to the Faraday-cup measurements is ±1.5%.

4. Background

The background, $n_b = n_{b1} + n_{b2}$, which fluctuated as much as 15%, determined the upper energy limit at which meaningful measurements could be made in H_2 and He. The effect on the points actually measured is significant only at low pressures and for the low-Z gases.

Estimates of the number of neutrals created in the residual gas account for virtually all of the neutral background (i.e., the contribution from collimator scraping appeared to be negligible). We therefore determine the fraction of neutrals produced ahead of the gas cell, n_{b1}/n_b, from drift-path lengths and estimate the value used, 0.8, to be accurate to ±10%.

5. Impurities

Chemical analysis of the target gases showed appreciable impurities to be present only in the case of hydrogen: 0.2% nitrogen, 0.004% CO_2, and 0.015% CO. These small concentrations are significant because their capture cross sections are larger than that of hydrogen by a factor of some 50 to 800 through our range of energies. The corrections to the hydrogen capture cross sections that must be applied because of these small amounts of heavy impurities range from 2% at the lowest energy to 17% at the highest energy. The errors in σ_{10} due to the uncertainty in these corrections are estimated to range between ±0.6% and ±5.1%.

The proton-energy-calibration uncertainties, which are important because of the strong energy dependence of σ_{10}, have been discussed in Section III.

C. Consistency of Measurements

Individual measurements of σ_{10} were made over a range of pressures. They were thus subject to various errors, but generally did not change with pressure, as would be the case for significant errors in our pressure calibrations, corrections for electron-loss collisions, or measurement of neutral background counts. Figures 2 and 3 show, respectively, plots of data with error bars for a typical set of measurements (N_2 at 0.851 MeV) and for a set (H_2 at 0.654 MeV) with high neutral background and high associated errors. In both cases, the weighted average is indicated at zero pressure.

D. Experimental Results

The measured loss and capture cross sections, σ_{01} and σ_{10}, are given in Tables I and II and are plotted in Figs. 4 through 7 for comparison with other experiments and with theoretical estimates.

V. DISCUSSION

Our values of σ_{01}, the ionization cross section, shown in Figs. 4 through 7 are in quite good agreement with measurements at both higher and lower energies, agreeing within the experimental error but, on the average, lying a little above the concensus of previous experiments. On the other hand, only for hydrogen and helium do the electron-capture cross sections σ_{10} agree within the experimental uncertainty with the results of Barnett and Reynolds[4] in the energy range where they overlap (440 keV to 1 MeV). In nitrogen and argon our values of σ_{10} are up to 50% larger than the Barnett and Reynolds results. We do not know the origin of this discrepancy.[38] There is good agreement with the previous high-energy measurements by Berkner et al.[5] for He, N_2, and Ar.

The theoretical curves plotted in Figs. 4 through 7 have been obtained by (a) raising the cross sections for capture into the ground state of hydrogen by 20% to allow for capture into all states (Section IIB), and (b) for the case of diatomic molecules (H_2 and N_2), doubling the atomic-capture cross sections. The size of the error associated with correction (b) is not known for our energy range, but the fact that there is a difference between atomic and molecular targets is demonstrated by the experimental work of McClure[39] with protons of 2 to 117 keV incident on H and H_2 targets. Below ~ 70 keV, σ_{10} for an atom is more than half of σ_{10} for a molecule, the reverse being true above about 70 keV. At 117 keV the atomic cross section is 40% of the molecular cross section. Tuan and Gerjuoy[40] have calculated that at very high energies $Q_{molecular} \rightarrow 2\gamma Q_{atomic}$ as a result of the higher electron momenta in the H_2 molecule. (The coefficient γ ranges between 1.2 and 1.4, depending on the molecular wave function used.) We would expect the atom-molecule discrepancy to be less important for higher Z.

A sampling of theoretical results of the types described in Section II is given in Fig. 4 to illustrate the spread in theoretical predictions. Shown are the Brinkman and Kramers (B-K) Born approximation, the Jackson and Schiff (J-S) Born approximation, a Bates-expansion calculation (Mc), and an impulse approximation by Cheshire (C1). Also shown are first-order (C2) and second-order (C3) distorted-wave calculations by Cheshire, and Mittleman's estimate (Mi) (see Section IIB).

The best chance for an accurate comparison between theory and experiment would seem to be in helium. In Fig. 5, Ma (1) is a B-K type calculation by Mapleton. The Jackson-Schiff-type approximation of Mapleton, Ma (2), agrees quite well with the experimental points, while the impulse-approximation calculations of Bransden and Cheshire (B-C) and the expansion calculation of Bransden and Sin Fai Lam[41] (B-SFL) bracket both the first Born calculation and the experimental points and differ from each other by about a factor of two. It is clear that the cross section is falling off more slowly than the E^{-6} curve labeled Mi at energies of a few MeV, but there are not enough data to give an asymptotic slope.

In the case of N_2 the apparent break in curvature found between our experimental results and those of Barnett and Reynolds suggests some structure to the σ_{10} curve near 1 MeV. The structure seems to be qualitatively explained by the B-K calculations of Mapleton, plotted in Fig. 6 as Ma (4), Ma (5), and Ma (6). Ma (4) includes only capture of 2p electrons of atomic nitrogen, Ma (5) includes 2s and 2p capture, and Ma (6) includes 1s, 2s, and 2p capture. Capture of p electrons is important at low energies but falls off asymptotically as E^{-7} at high energies, where s-orbital capture, which asymptotically falls off as E^{-6}, predominates. It appears, therefore, that the observed changes in curvature may be attributable to differing dominant capture reactions at different energies. Ma (3) is the first Born (Jackson-Schiff) result obtained in the approximate way described in Section IIB. Mittleman's expression, which for nitrogen is just entering his suggested range of validity at our highest energy, gives a result that is in reasonably good agreement with experiment, but measurements at still higher energies are required before a comparison with his predicted energy dependence can be made.

The argon data of Fig. 7 show a structure similar to, but more pronounced than, that in N_2. This suggests that the effect of capturing different orbital electrons is probably present also in argon. We do not know of any theoretical work applicable to argon in this energy range except the classical work of Thomas and Bohr. For energies between 2.5 and 13.75 MeV the N_2 and Ar experimental curves have energy dependences of approximately $E^{-4.5}$ and $E^{-3.9}$, respectively, which are not too different from the classical predictions.

In conclusion, it seems clear that the experiments to date now provide a basis for comparison with various calculations, but additional measurements at very high energies are still necessary.

ACKNOWLEDGMENTS

We wish to thank Dr. C. M. Van Atta for his support of this research. One of us (SNK) would also like to express his appreciation to Professors B. J. Moyer and A. C. Helmholz for their support during the course of this work. Much valuable assistance was extended in the assembly and operation of equipment by J. Warren Stearns, Vincent J. Honey, and John C. Warren. We are indebted to Dr. M. H. Mittleman for his participation in several fruitful discussions and for his comments on the manuscript. LMW was supported by the U. S. Air Force.

FOOTNOTES AND REFERENCES

*This work was done under the auspices of the U. S. Atomic Energy Commission.

†Major, USAF, present address: Directorate of Science and Technology, Deputy Chief of Staff for Research and Development, Headquarters USAF, Washington, D. C.

1. L. H. Thomas, Proc. Roy. Soc. (London) A114, 561 (1927).
2. H. C. Brinkman and H. A. Kramers, Proc. Acad. Sci. Amsterdam 33, 973 (1930).
3. See, for example, the review article by S. K. Allison and M. Garcia-Munoz, in Atomic and Molecular Processes, D. R. Bates (ed.) (Academic Press, New York and London, 1962).
4. C. F. Barnett and H. K. Reynolds, Phys. Rev. 109, 355 (1958).
5. K. H. Berkner, S. N. Kaplan, G. A. Paulikas, and R. V. Pyle, Phys. Rev. 140, A729 (1965).
6. R. Szostak, M. Martin, and P. Marmier, Helv. Phys. Acta 34, 485 (1961).
7. N. F. Mott and H. S. W. Massey, The Theory of Atomic Collisions, Third Edition (Oxford University Press, London, 1965), p. 618.
8. B. H. Bransden and I. M. Cheshire, Proc. Phys. Soc. (London) 81, 820 (1963).
9. M. H. Mittleman, Proc. Phys. Soc. (London) 81, 633 (1963).
10. D. R. Bates and R. McCarroll, Advan. Phys. 11, 39 (1962).
11. B. H. Bransden, in Advances in Atomic and Molecular Physics (Academic Press, New York and London, 1965), Vol. I.

12. D. R. Bates and R. A. Mapleton, Proc. Phys. Soc. (London) 87, 657 (1966).

13. C. J. Cook, Proc. Phys. Soc. (London) 81, 789 (1963).

14. N. Bohr, The Penetration of Atomic Particles Through Matter (I Kommission Hos E. Munksgaard, København, 1948).

15. Michal Gryzinski, Phys. Rev. 138, A336 (1965).

16. J. R. Oppenheimer, Phys. Rev. 31, 349 (1928).

17. J. D. Jackson and H. Schiff, Phys. Rev. 89, 359 (1953).

18. R. A. Mapleton, Phys. Rev. 130, 1839 (1963); Phys. Rev. 122, 528 (1961).

19. R. A. Mapleton, Proc. Phys. Soc. (London) 85, 1109 (1965); Phys. Rev. 130, 1829 (1963).

20. R. A. Mapleton, Phys. Rev. 145, 25 (1966).

21. The Z dependence as originally given in Ref. 9, Eq. (23), is incorrect; M. H. Mittleman, Space Sciences Laboratory, University of California, Berkeley (private communication).

22. We have used the following values for $n_A(0)$ for the curves shown in Figs. 4 through 6: π^{-1} for H; 3.62 for He; and 208. for N.

23. M. H. Mittleman, Space Sciences Laboratory, University of California, Berkeley (private communication).

24. R. A. Mapleton, Phys. Rev. 126, 1477 (1962).

25. Richard M. Drisko, The Theories of Positronium and of Rearrangement Collisions, Thesis, Carnegie Institute of Technology, 1955 (unpublished). See Refs. 9 and 26.

26. R. Aaron, R. D. Amado, and B. W. Lee, Phys. Rev. 121, 319 (1961).

27. I. M. Cheshire, Proc. Phys. Soc. (London) 82, 113 (1963).

28. T. Pradhan and D. N. Tripathy, Phys. Rev. 130, 2317 (1963); T. Pradhan, Phys. Rev. 105, 1250 (1957).

29. D. R. Bates, Proc. Roy. Soc. (London) A247, 2941 (1958).

30. R. McCarroll, Proc. Roy. Soc. (London) A264, 547 (1961).

31. I. M. Cheshire, Proc. Phys. Soc. (London) 84, 89 (1964).

32. There is the implicit assumption in this approach that the σ_{01} cross section obtained in this way is the same as σ_{01} averaged over excited states of the H^0 atoms within the gas neutralizing cell. It is known that σ_{01} increases somewhat with the principal quantum number, n, and that the distribution over excited states depends on the type of neutralizer and on radiative decay between the neutralizer and the gas cell. However, the fact that we get the same values of σ_{10}, independent of neutralizing gas pressure, indicates that no significant error is made.

33. K. H. Berkner, S. N. Kaplan, and R. V. Pyle, Phys. Rev. 134, A1461 (1964).

34. C. Meinke and G. Reich, Vacuum 13, 579 (1963).

35. V. J. Ashby and M. A. Williamson, revised by Rex Booth, Cyclotron Range-Energy Measurement Instructions, Lawrence Radiation Laboratory, Livermore, Physics Division report Nu. Ph. 123, Rev. 1, April 20, 1959 (unpublished).

36. Jerry B. Marion, Accelerator Energy Calibrations, Rev. Mod. Phys. 33, 139 (1961).

37. R. Smythe and J. W. Toevs, Phys. Rev. 139, A15 (1965).

38. Recent remeasurements for these four gases in the energy range 100 to 550 keV are reported to agree, within the experimental uncertainties. L. M. Toburen, R. A. Langley, C. F. Barnett, R. D. Birkhoff, and M. I. Nakai, Bull. Am. Phys. Soc., Ser. II, 11, 818 (1966).

39. G. W. McClure, Phys. Rev. 148, 47 (1966).

40. T. F. Tuan and E. Gerjuoy, Phys. Rev. 117, 756 (1960).

41. B. H. Bransden and L. T. Sin Fai Lam, Proc. Phys. Soc. (London) 87, 653 (1966).

Table I. Electron-loss cross sections, σ_{01}. All values have standard errors of ±10%, due chiefly to uncertainties in gas target thickness.

	σ_{01} (10^{-17} cm^2/molecule)			
E (MeV)	H_2	He	N_2	Ar
1.027	2.2	1.5	17.	17.6
2.44	0.85	0.63	7.2	8.9

Table II. Electron-capture cross sections, σ_{10}.

Proton energy (MeV)	σ_{10}			
	H_2 (cm^2/molecule)	He (cm^2/atom)	N_2 (cm^2/molecule)	Ar (cm^2/atom)
0.440±0.003	$(3.6\pm0.4) \times 10^{-20}$	$(1.6\pm0.2) \times 10^{-19}$	$(9.8\pm1.1) \times 10^{-19}$	$(5.8\pm0.6) \times 10^{-19}$
0.654±0.003	$(4.0\pm0.6) \times 10^{-21}$	$(2.9\pm0.4) \times 10^{-20}$	$(2.5\pm0.3) \times 10^{-19}$	$(2.7\pm0.4) \times 10^{-19}$
0.851±0.004	$(1.1\pm0.12) \times 10^{-21}$	$(8.3\pm1.0) \times 10^{-21}$	$(9.8\pm1.1) \times 10^{-20}$	$(1.5\pm0.2) \times 10^{-19}$
1.063±0.006	$(3.5\pm0.5) \times 10^{-22}$	$(2.9\pm0.4) \times 10^{-21}$	$(5.1\pm0.6) \times 10^{-20}$	$(8.9\pm1.0) \times 10^{-20}$
2.45±0.03	$(6.0\pm1.4) \times 10^{-24}$	$(3.2\pm0.4) \times 10^{-23}$		
2.51±0.03			$(2.1\pm0.2) \times 10^{-21}$	$(4.3\pm0.5) \times 10^{-21}$
2.99±0.04		$(1.2\pm0.1) \times 10^{-23}$		
4.79±0.05			$(1.4\pm0.2) \times 10^{-22}$	$(3.2\pm0.4) \times 10^{-22}$
5.41±0.05		$(5.4\pm0.6) \times 10^{-25}$		
13.8 ±0.2			$(9.9\pm1.1) \times 10^{-25}$	$(5.5\pm0.6) \times 10^{-24}$

FIGURE LEGENDS

Fig. 1. Experimental arrangement.

Fig. 2. Plot of individual measurements and standard errors for σ_{10} in N_2 at 0.851 MeV. Systematic errors in the target thickness, Π, are not included.

Fig. 3. Plot of individual measurements and standard errors for σ_{10} in H_2 at 0.654 MeV. Systematic errors in the target thickness, Π, are not included.

Fig. 4. H_2 cross sections. Experimental results: ▮ present measurements; o Barnett and Reynolds (Ref. 4); ◇ Berkner et al. (Ref. 33); □ Smythe and Toevs (Ref. 37). Theoretical results: B-G, D. R. Bates and G. W. Griffing, Proc. Phys. Soc. (London) A65, 90 (1955); D-N, I. S. Dmitriev and V. S. Nikolaev, Soviet Physics-JETP 17, 447 (1963); Mi, Mittleman (Ref. 9); B-K, Brinkman and Kramers (Ref. 2); Mc, McCarroll (Ref. 30); P-T, Pradhan and Tripathy (Ref. 28); J-S, Jackson and Schiff (Ref. 17); C2 and C3, Cheshire (Ref. 31); C1, Cheshire (Ref. 27). The theoretical curves were obtained by multiplying calculations for capture into 1s states from atomic hydrogen by 2×1.20.

Fig. 5. He cross sections. Experimental results: ▮ present measurements; o Barnett and Reynolds (Ref. 4); ◇ Berkner et al. (Ref. 33); □ Smythe and Toevs (Ref. 37); ◊ Berkner et al. (Ref. 15). Theoretical results: B-W, D. R. Bates and A. Williams, Proc. Phys. Soc. (London) A68, 90 (1955); D-N, Dmitriev and Nikolaev (see Fig. 4 caption); Mi, Mittleman (Refs. 9, 21, and 22); B-SFL, Bransden and Sin Fai Lam (Ref. 41); Ma (1)

and Ma (2), Mapleton (Ref. 18); B-C, Bransden and Cheshire (Ref. 8). Theoretical calculations for capture into the 1s state have been multiplied by 1.20.

Fig. 6. N_2 cross sections. Experimental results: | present measurements; o Barnett and Reynolds (Ref. 4); ⬭ Berkner et al. (Ref. 33); □ Smythe and Toevs (Ref. 37); △ R. Szostak, M. Martin, and P. Marmier, Helv. Phys. Acta 34, 485 (1961); ◊ Berkner et al. (Ref. 5). Theoretical results: Ma (3), Ma (4), and Ma (5), Mapleton (Ref. 19); Ma (6), Mapleton (Ref. 20); Mi, Mittleman (Refs. 9, 21, and 22). The theoretical curves were obtained by multiplying calculations for capture into 1s states from atomic nitrogen by 2 × 1.20.

Fig. 7. Ar cross sections. Experimental results: | present measurements; o Barnett and Reynolds (Ref. 4); ⬭ Berkner et al. (Ref. 33); □ Smythe and Toevs (Ref. 37); ◊ Berkner et al. (Ref. 5).

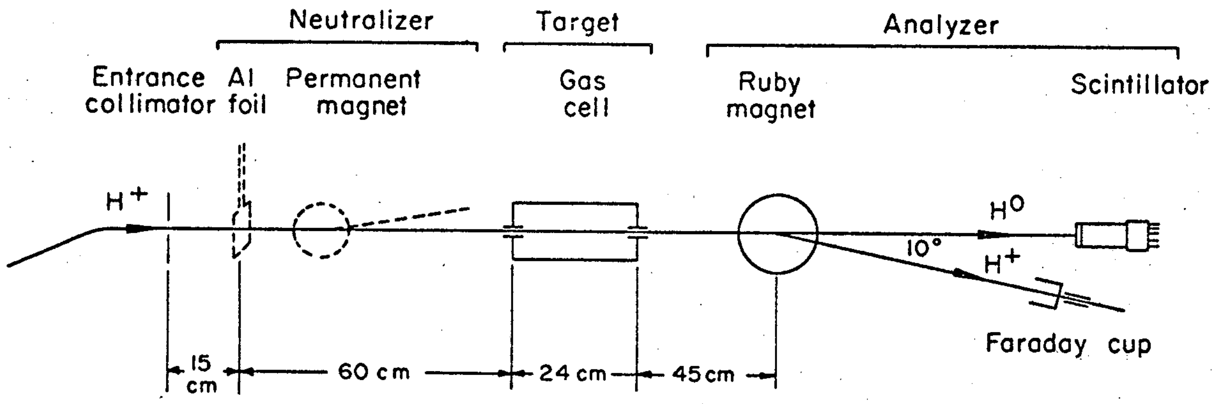

Fig. 1

MUB-10397

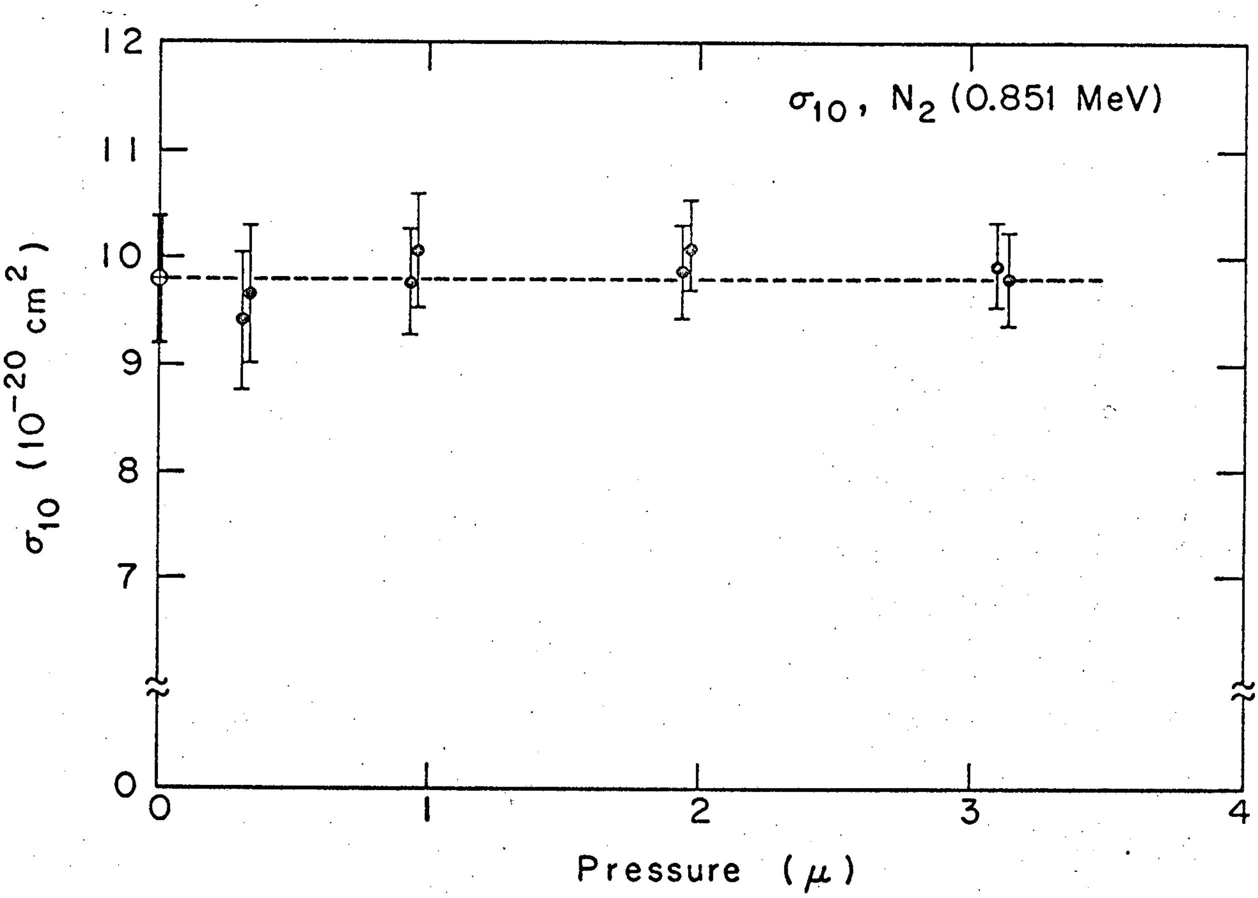

Fig. 2

MUB-10670

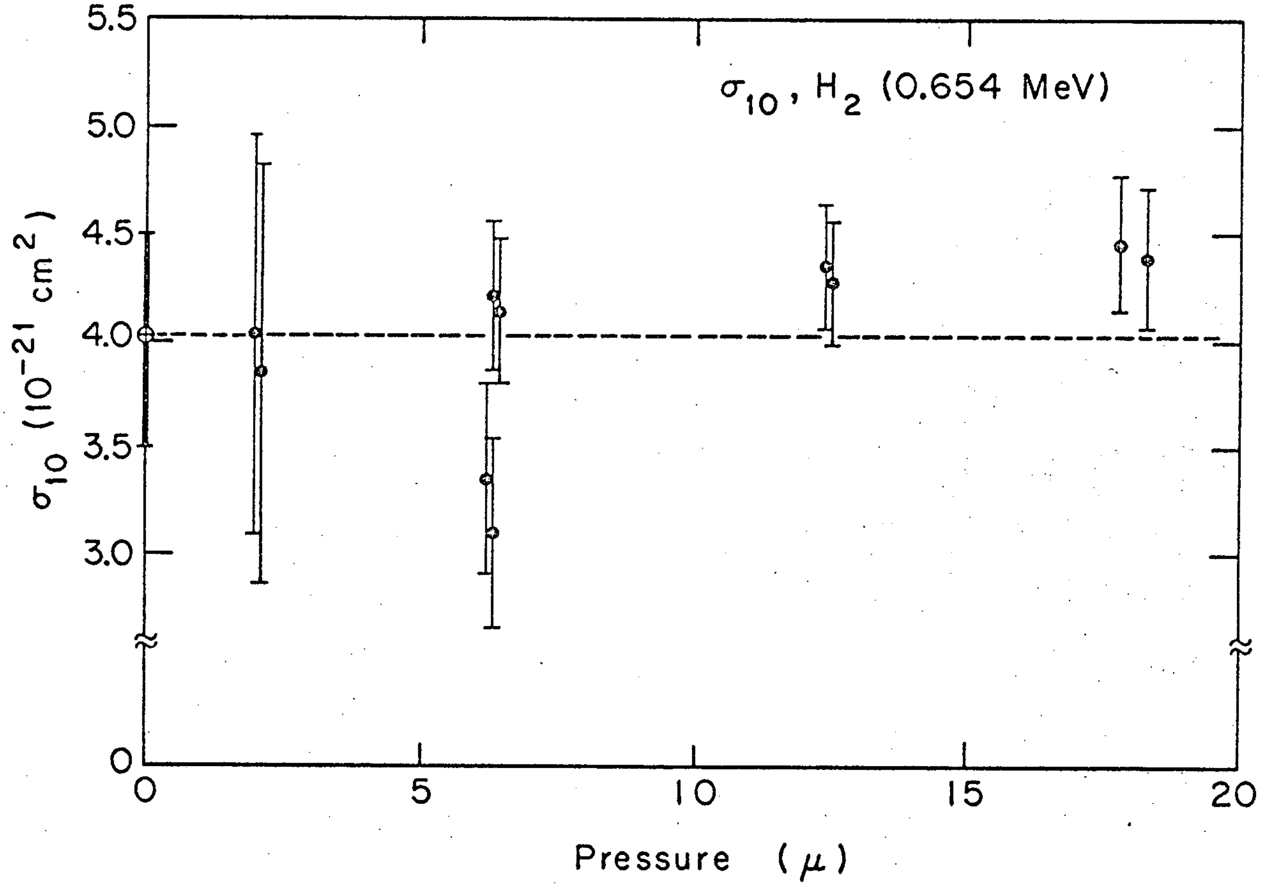

Fig. 3

MUB-10671

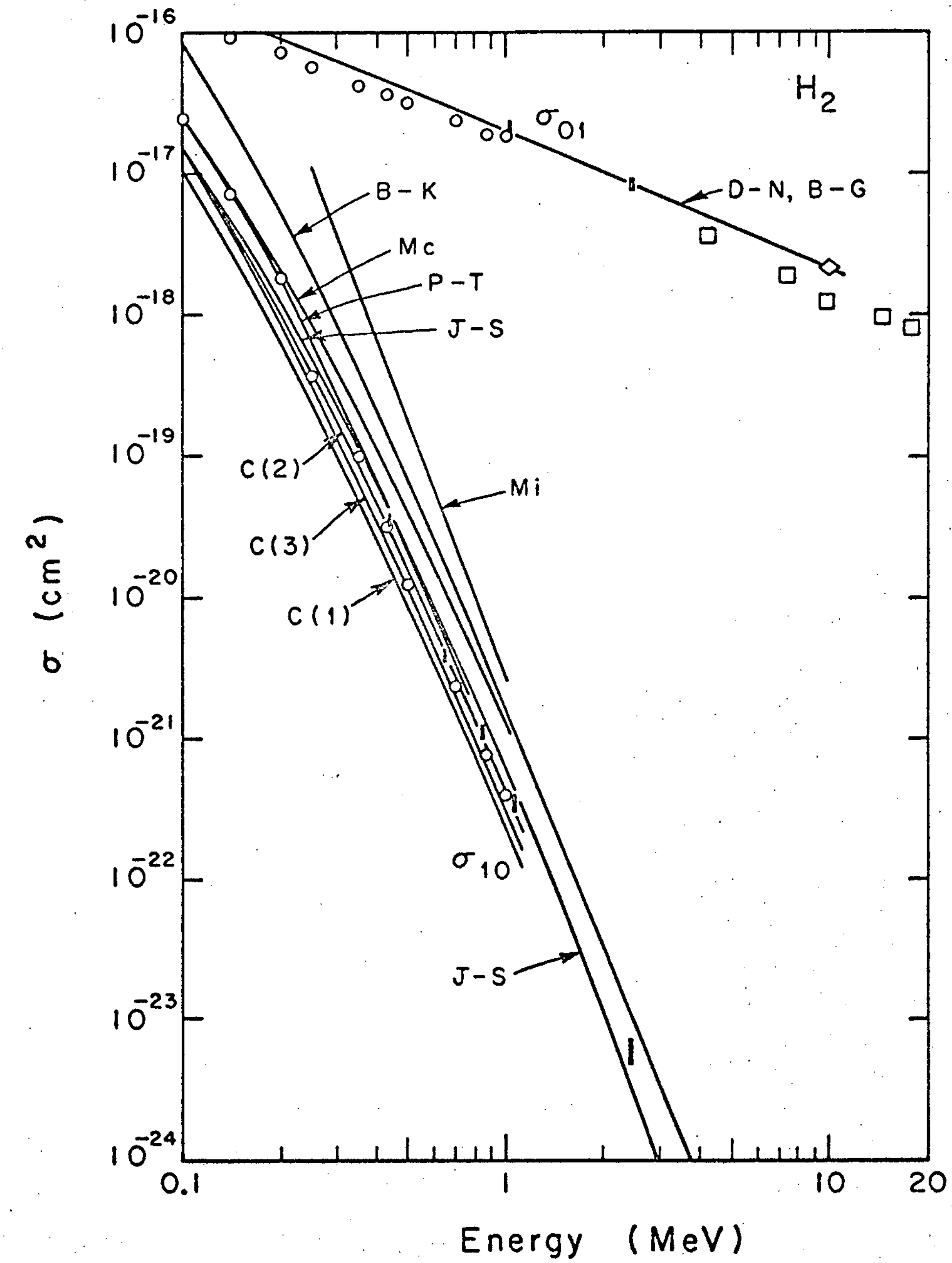

Fig. 4

MUB-10672

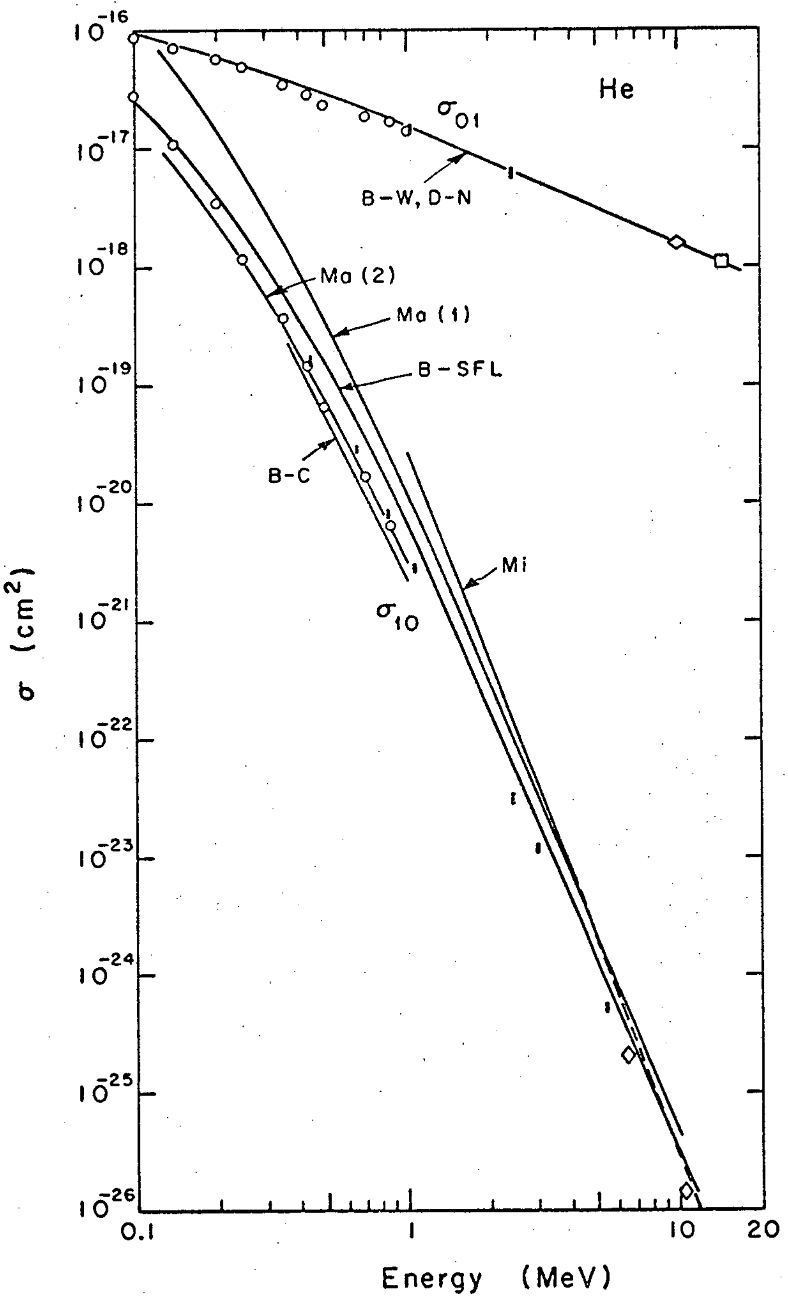
He
σ_{01}
B-W, D-N
Ma (2)
Ma (1)
B-SFL
B-C
Mi
σ_{10}
10^{-16}
10^{-17}
10^{-18}
10^{-19}
10^{-20}
10^{-21}
10^{-22}
10^{-23}
10^{-24}
10^{-25}
10^{-26}
σ (cm^2)
0.1
1
10
20
Energy (MeV)
MUB-10673

Fig. 5

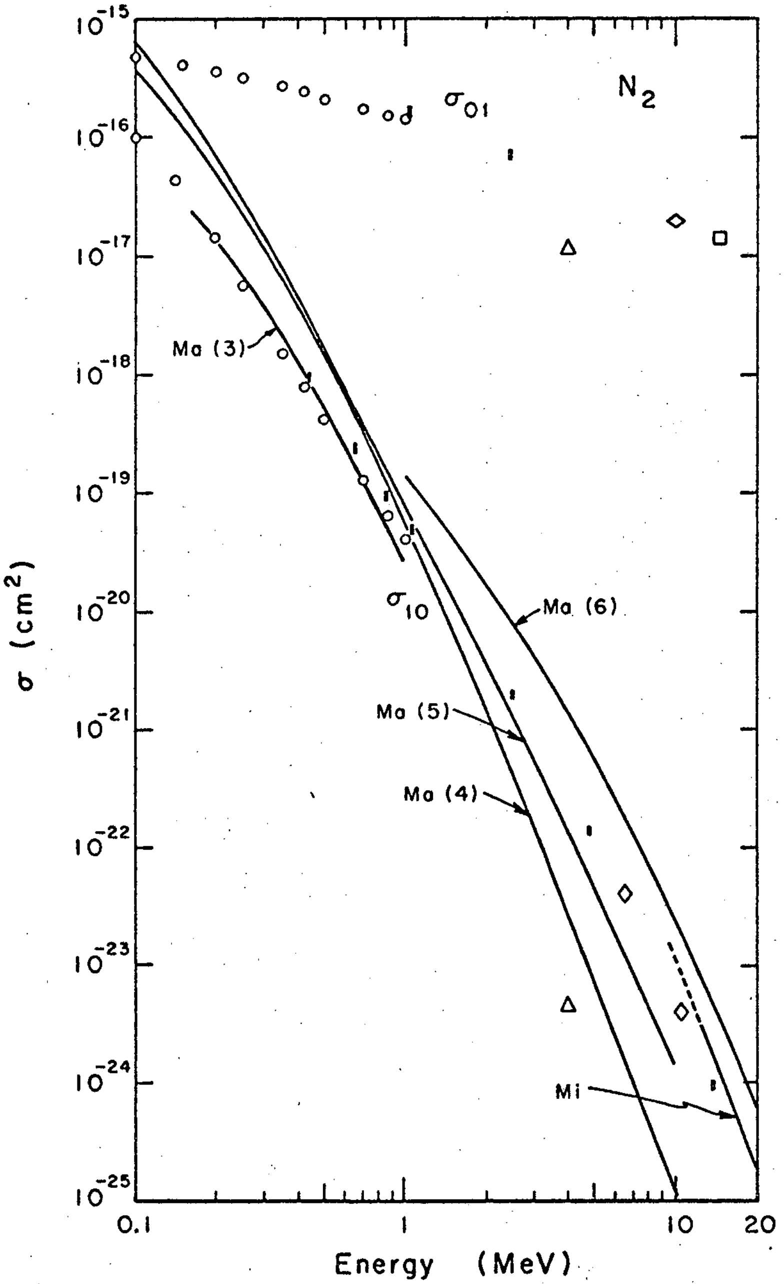

Fig. 6

MUB-10668

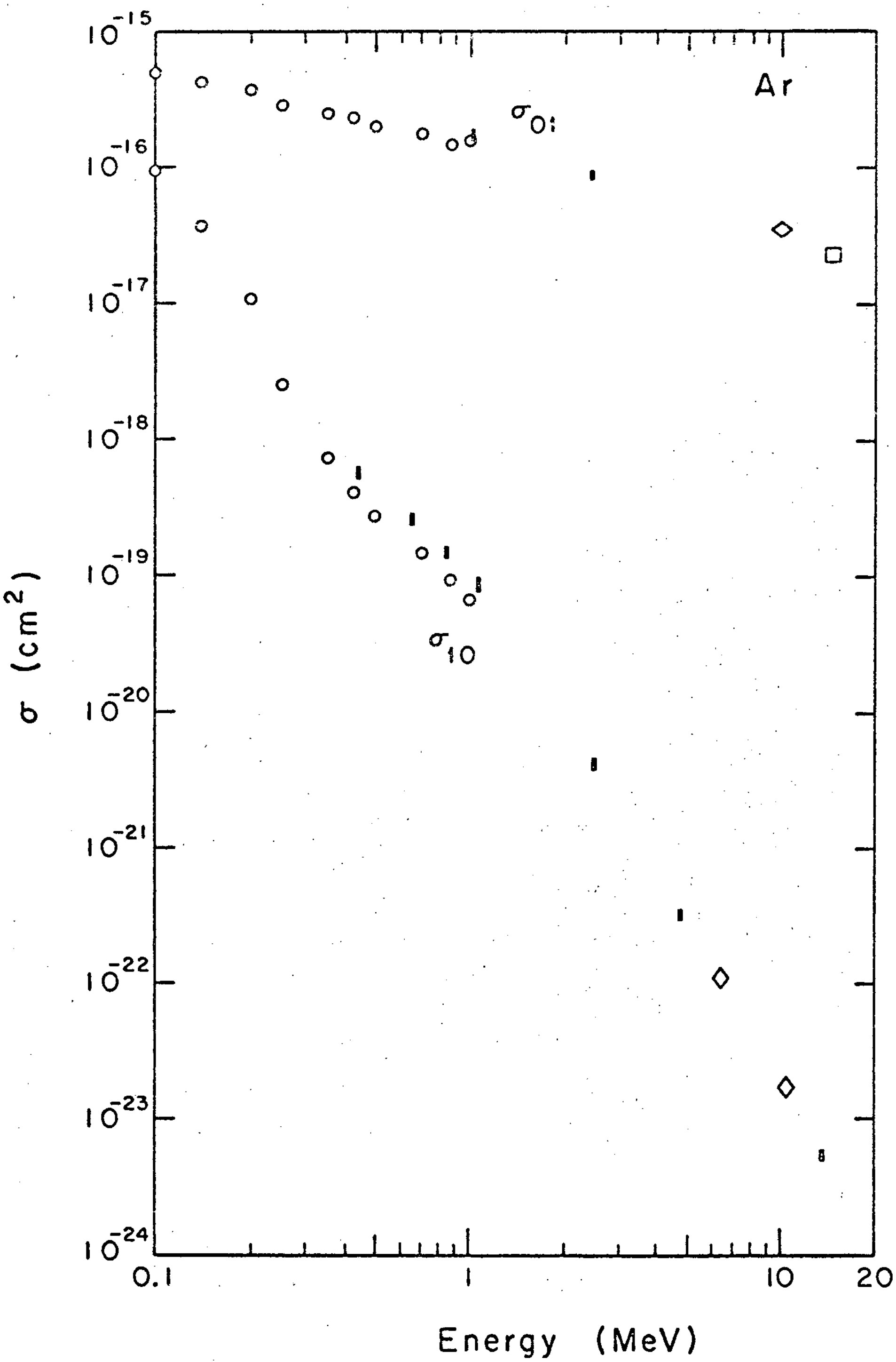

Fig. 7

MUB-10669